Catalysis Letters 7 (1990) 61–82

CARBIDE PHASES ON IRON-BASED FISCHER-TROPSCH SYNTHESIS CATALYSTS
PART I: CHARACTERIZATION STUDIES

John B. BUTT

Ipatieff Laboratory and Department of Chemical Engineering, Northwestern University, Evanston, IL 60208-3120, U.S.A.

Synthesis catalysts, characterization of, Mössbauer spectra, iron alloy catalysts, X-ray diffraction, iron alloy catalysts, XPS spectra, iron synthesis catalysts.

The characterization of iron carbide phases formed on iron-based Fischer-Tropsch catalysts is reviewed in this part with particular emphasis on Mössbauer and XPS studies of selected iron and supported iron catalysts, in combination with some specific results in activity and selectivity. Mössbauer studies have shown clearly the evolution of bulk carbide species on iron catalysts under synthesis reaction conditions; the relationship of these to the nature of near-surface species and their temporal evolution under synthesis conditions is indicated by XPS results. Comparisons among reduced, unreduced and carbided iron catalysts are given; XPS and reaction results suggest that Fe_3O_4 is active for synthesis even in the absence of carbide phases.

1. Introduction

The potential importance of carbide phases on the operation of iron-based Fischer-Tropsch catalysts has been recognized for a long time. However, the quantitative characterization of the nature of these phases and their importance in determination of synthesis activity/selectivity patterns has been accomplished only relatively recently. This part presents an overview of the formation and characterization of carbide phases on supported iron and iron alloy catelysts. The literature is substantial, so the presentation is selective rather than comprehensive.

2. Formation and characterization of carbide phases–supported iron

The results of a considerable amount of work on iron catalysts can be summarized rather compactly. Such catalysts in all forms (precipitated, fused and supported) are rather readily converted to one or more carbides under FT reaction conditions; the more recent work has employed Mössbauer spectroscopy,

X-ray diffraction (XRD), thermomagnetic analysis and X-ray photoelectron spectroscopy (XPS) to study carbide formation [1–7]. For bulk iron the carbides formed are a mixture of ε'-$Fe_{2.2}C$ and χ-Fe_5C_2 phases [3] and for supported materials primarily the ε'-$Fe_{2.2}C$ [1,2] and χ-Fe_5C_2 phases (see later). Carbide formation is generally accompanied by increased activity, and this interrelationship has been interpreted in terms of a "competition model" in which the formation of carbide phases and hydrocarbon products involve a common carbon intermediate. For supported iron the carbide phase is formed over a relatively short period of time, and the accompanying change in activity can be quite significant. Fig. 1 gives typical data for a 4.94 wt.% Fe/SiO_2 catalyst with 8.1% Fe exposed after reduction in H_2, 425 °C, 24 h. This, and other early work on characterization of carbide formation made extensive use of Mössbauer spectroscopy, since the phase change from one carbide to another involves only small changes in iron position and stoichiometry. Arents et al. [8] have characterized the Mössbauer spectra of the various iron carbides, and their results are listed in table 1 together with the appropriate crystallographic data. As seen, the ε, χ, χ' and χ'' carbides each contain three distinct six line spectra in the Mössbauer pattern, while the ε' and Θ appear as single six line patterns. Phase identification is based on the number of six-line spectra observed, their hyperfine magnetic field (H), and their relative intensities. As might be inferred from this and from the number of possible carbide phases, it has taken some time to obtain agreement that the carbide phase formed on supported Fe is primarily ε'-$Fe_{2.2}C$. Even at this, a long line of qualifiers applies, since most reaction data on which this conclusion is based are at low total conversions of CO, atmospheric pressure, moderate temperatures (250–300 °C) and a molar feed stoichiometry of $1/3 = CO/H_2$. An early appreciation of the carbide problem for unsupported catalysts has been given by Anderson [11], where the χ-Fe_5C_2 phase is also of importance.

Even the impressive assembly of information in table 1 does not tell the whole story for Mössbauer characterization, however, for those data pertain to room temperature characterization. More information is obtained if the spectra are recorded at liquid-N_2 and liquid-He temperatures [12]. In earlier work, Niemanstverdriet et al. [3] noted evidence for an "oxide" spectrum in the 4.2 K pattern for a carburized iron catalyst ($CO + H_2$ at 250 °C) that had been exposed to air. In order to resolve this problem, Mössbauer spectra at other temperatures were investigated. We thus should expand on the information given in table 1 to include relevant data, as shown in table 2. Also included in the table are values for isomer shift relative to iron, δ, and magnetic hyperfine splitting, ΔE_Q (see also ref. [13].) The "oxide" noted in [3] was identified as either γ-FeOOH or an amorphous iron gel that resulted from exposure of the carburized catalyst to air and not to some oxidation reaction occurring during the synthesis. However, the spectra at different temperatures required to resolve the oxide question complicated the carbide question, since the additional detail provided in the Mössbauer patterns revealed the presence of a considerable amount of χ-Fe_5C_2

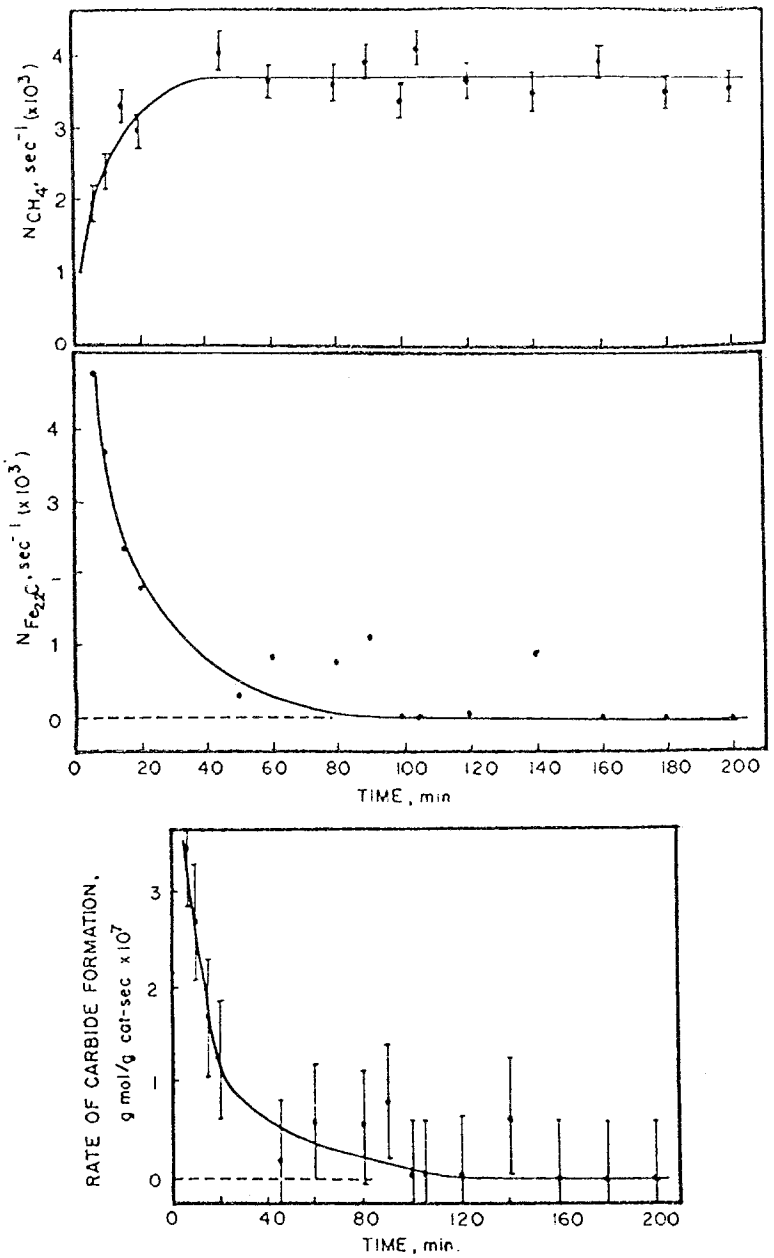

Fig. 1. Change in activity and rate of carbide formation in a supported iron catalyst [1]. $T = 255\,^{\circ}C$, $CO/H_2 = 1/3$.

(~ 45%). For the record, the Mössbauer patterns and associated parameters of this determination are given in table 3 and fig. 2, respectively.

To repeat a warning above, however, the generality of such results must be carefully qualified, not only as to the system of iron dispersed on an inert

Table 1
Some properties of iron carbides

Carbide	Crystal structure	Curie temperature (°C)	Magnetic iron positions	H (kOe)	Relative population of position	Formula	Lattice constants (Å)	
ε	HCP	380±10	I	170±3	4	Fe_2C	$a = 4.767$	$a = 2.73$
			II	237±3	1.6		$b = 4.354$	$b = 4.33$
			III	130±6	1		(Ref. [9]	(Ref. [10]
ε'	HCP ↓ Monoclinic	450±10	I	170±3	–	$Fe_{2.2}C$	–	
χ	Monoclinic	232±10	I	184±3	2	Fe_5C_2	$a = 11.562$	$c = 5.0595$
			II	222±3	2		$b = 4.5727$	$\beta = 94.74°$
			III	110±6	1			
χ'	Monoclinic ↓ Orthorhombic	220±10	I	203±3	2	–	–	
			II	214±3	1.8			
			III	118±6	1			
χ''	Monoclinic ↓ Orthorhombic	210±10	I	195±3	1	–	–	
			II	214±3	2			
			III	118±6	1			
θ	Orthorhombic	208± 3	I	208±3	1	Fe_3C	$a = 5.0896$	
			II	208±3	2		$b = 6.7443$	
							$c = 4.5248$	

Table 2
Selected Mössbauer parameters

Material	δ (mm/s)	ΔE_Q (mm/s)	H (kOe)	Temperature
α-Fe	0.0	0.0	333	room
	0.11	0.0	343	liq He
α-Fe_2O_3	0.36	0.24	515	room
ε'-$Fe_{2.2}C$	0.25	−0.11	170	room
χ-Fe_5C_2	0.23	0.08	216	room
	0.37	0.16	248	liq N_2
	0.38	0.16	252	liq He
β-FeOOH	–	–	490	liq He
γ-FeOOH	–	< 0.1	460	liq He
Fe "gel"	0.4	0.0	480	liq He

Table 3
Temperature dependence of Mössbauer parameters for supported Fe–carburized 24 h, 300 °C and air passivated

Temperature	Component	δ (mm/s)	ΔE_Q (mm/s)	H (kOe)	Area fraction and $\chi/(\chi+\varepsilon')$	
room	ε' carbide	0.25 ± 0.03	-0.11 ± 0.03	173 ± 3	–	0.23
	χ carbide	0.24	−0.12	218	–	–
liquid N_2	ε' carbide	0.38	−0.13	188	0.71	0.43
	χ carbide	0.40	−0.15	249	0.15	–
	"oxide"	0.39	1.09	–	0.14	–
liquid He	ε' carbide	0.38	−0.13	191	0.38	–
	χ carbide	0.37	−0.26	252	0.30	0.44
	"oxide"	0.45	0.04	470	0.32	–

support, but as to numerous other factors. For sufficiently high dispersion (small metal particle sizes), for example, one would expect carbide formation to be suppressed if for no other reason than there are fewer places for the carbon to go. The relative stability of the various carbides is apparently affected by the CO/H_2 ratio [9,14], particle size and strain [8], and the extent of reduction to metallic iron [11,15].

As a final note in this section, the nature of the iron and/or iron oxide on the silica supported catalyst detailed in table 3 should be examined. This catalyst was prepared by impregnation to incipient wetness from aqueous $Fe(NO_3)_3$ onto Davison grade 62 silica gel (340 m^2/g, 14 nm average pore diameter). After calcination at 450 °C for 4 h, the iron exists on the SiO_2 as well defined α-Fe_2O_3 [1,16]. XRD analysis using the conventional Scherrer approach gave an average oxide crystallite size of ~ 18 nm, while use of the more sophisticated Fourier line profile analysis gave a particle size of ~ 10 nm. The particle size distribution obtained from Fourier analysis was very broad (2–16 nm) with a mean value of about 8 nm. When X-ray analysis indicates a broad particle size distribution, it is wise to utilize other methods for physical characterization. Transmission electron microscopy (TEM) examination of the oxide reveals a physical picture considerably different from that of XRD. In fact, the α-Fe_2O_3 has a particle size much larger (~ 80 nm) than that determined by XRD, and the oxide aggregate appears to be a single crystallite (although filled with faults such as low-angle grain boundaries). Also in view of the ~ 14 nm pore diameter of the silica, the oxide particle size obviously has little relation to the pore structure of the support. Thus, before reduction we have large α-Fe_2O_3 "clumps" consisting of highly imperfect single crystals that consist of coherently diffracting domains [16]. What happens when this catalyst is reduced? After H_2, 425 °C, 24 h the faulted single crystal is ruptured into a grape-cluster structure in which the metal particles are in close contact with each other. The metal particle sizes are perhaps somewhat

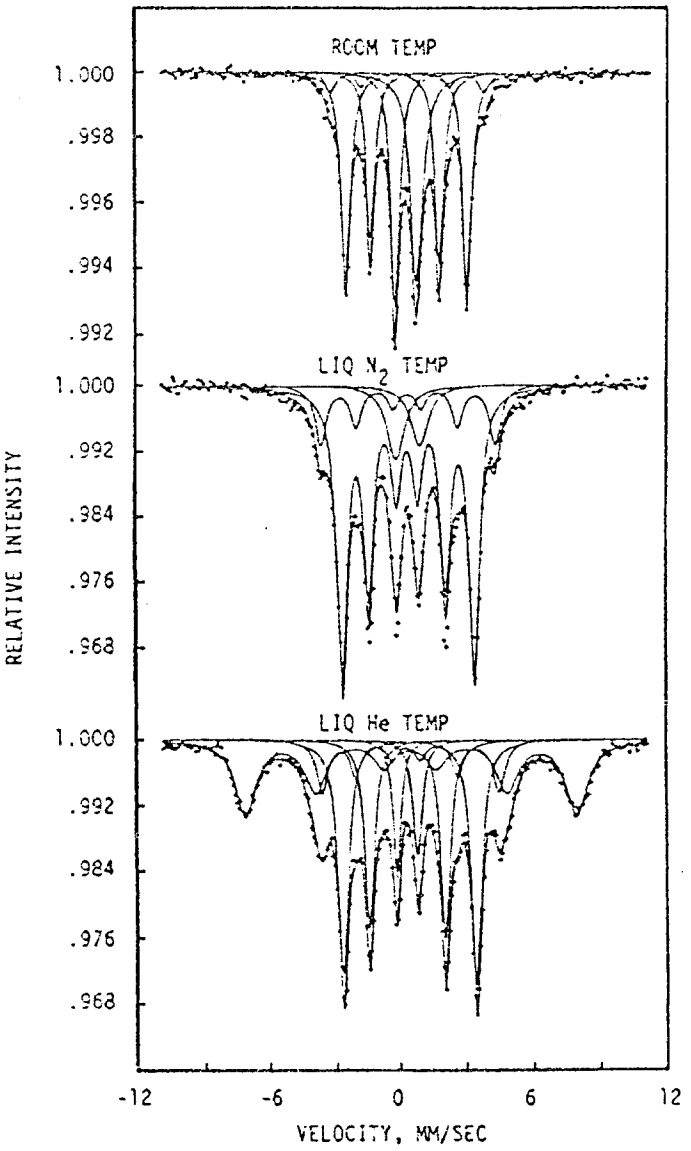

Fig. 2. Room-, liquid N_2- and liquid He-temperature spectra of passivated-carbided iron.

smaller than those of the initial oxide domains. However, the exposed surface area of the reduced metal that is accessible to hydrogen chemisorption is considerably lower than that expected from XRD, probably because of contact among the metal crystallites. The relatively large size of the reduced iron crystallites is probably an important factor in the formation of χ-Fe_5C_2 (reminiscent of bulk iron) in such materials, and one should in principle be able to alter the ratio of carbides formed (ε' to χ) by changing particle size. This is easily accomplished in catalyst preparation step, since the precursor large oxide clumps

are formed in the calcination procedure. If the freshly impregnated wet metal nitrate catalyst is directly calcined at 500 ° C for 1 h a dispersed particulate oxide phase is formed consisting of discrete crystallites with an approximate dimension of 8–10 nm. Presumably such procedures could be further modified to give yet other oxide precursor particle sizes, and a wide range of (ε'/χ) ratios produced. This approach, however, does not appear to have been reported in the literature.

3. Formation and characterization of carbide phases–selected supported iron alloys

Some time ago Dry et al. [17] proposed that the action of well known alkali promoters such as potassium had the net effect of increasing the heat of chemisorption of CO on reduced iron catalysts. It was postulated that such

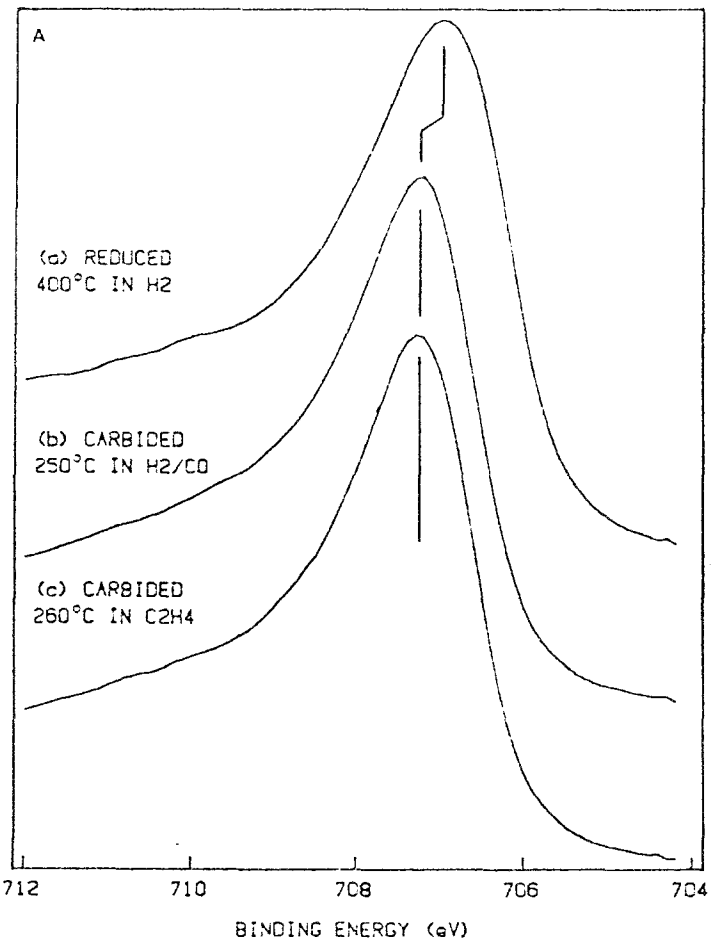

Fig. 3. Iron core-level spectra for reduced and carbided powder samples. (A) Fe ($2p_{3/2}$), (B) Fe (3p).

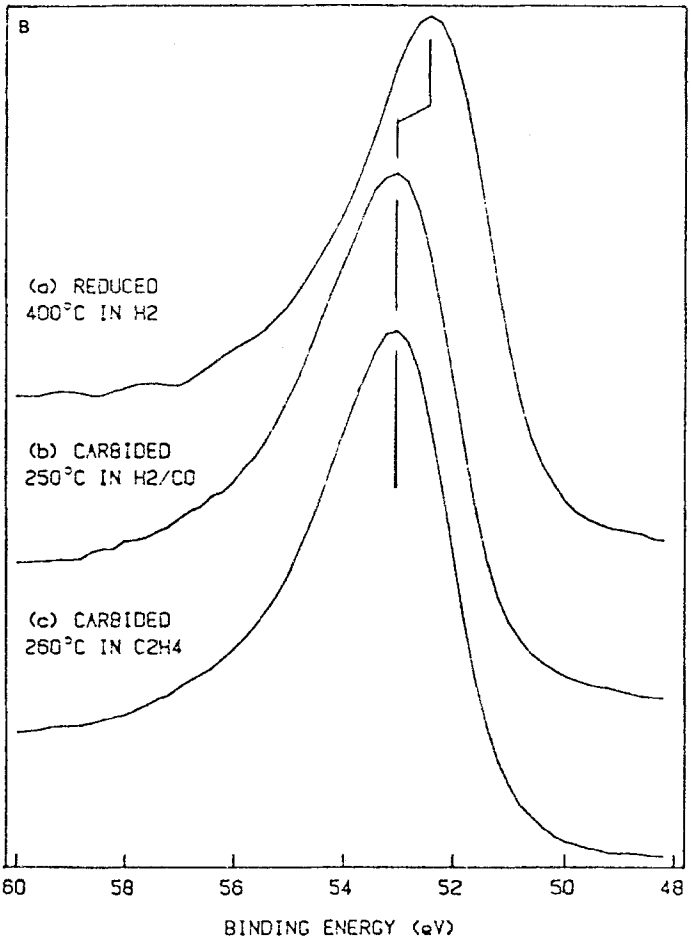

Fig. 3. (continued).

promotion occurs by donation of electrons from K to Fe that in turn increases the donation of electrons from iron to the antibonding orbital of CO upon its adsorption. The argument was extended by Vannice and Garten [18] to supported Fe-Pt bimetallic catalysts. In this instance, Pt should withdraw electrons from the iron and hence one should observe a decrease in activity relative to pure Fe. However, formation of carbides can alter this picture substantially. K-promoted iron forms carbides under synthesis conditions [11,19], and it may be true that potassium also donates electrons to the carbide. However, in the Fe-Pt system, alloy formation can suppress the formation of carbides [20], there could be enhanced activation of hydrogen, and the working catalyst would in several ways be quite different from Fe.

This general line of reasoning concerning the possible action of Fe-based alloys has been applied in selection of a number of potential catalysts systems for study

of FT activity and selectivity by a number of laboratories over the past decade or so. The experience of this laboratory is typical, as described in the following.

Following the experience described in refs. [17,18], some typical alloy systems to examine in terms of electronic promotion and carbide formation were selected as Fe-Ni, Fe-Co, and Fe-Cu, along with further study of Fe-K. A number of these catalysts were prepared via aqueous impregnation ex nitrate solution (potassium ex carbonate) onto SiO_2, most to a weight level (total metals) ca. 5.0% and Fe/M ~ 4. One would expect Co and Ni to have only small effects on the electronic structure of iron in the alloy [20] and render the carbide phase less stable. If electronic effects were observed, Co would probably show a larger effect, while Ni may have the stronger effect for hydrogen activation. The expectation for Fe-Cu would be that of no interaction other than dilution. Finally, one would look to see if K-promotion for supported iron is similar to that for the bulk phase.

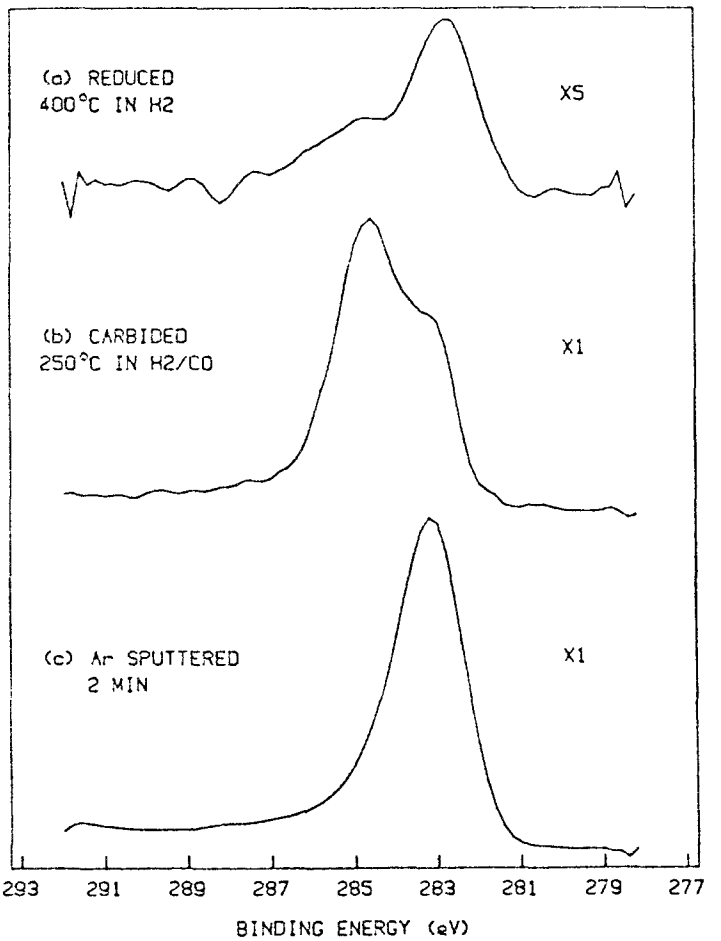

Fig. 4. C (1s) XPS spectra of reduced and carbided iron foil.

Table 4
Binding energy data. References as in [5]

Binding energy data for metallic iron

Ref.	$Fe(2p_{1/2})$	$Fe(2p_{3/2})$	Fe(3d)	Fe(3p)
[22]	–	707.0	–	–
[10]	720.3	707.3	–	–
[12]	721.6	708.6	91.6	53.1
[17]	720.2	707.3	–	53.2
[20]	719.9	706.8	91.4	52.9
[21]	–	706.9	90.9	53.0
[27]	–	706.6	–	–
[31]	–	706.5	–	–

Binding energy data for Fe_xO

Ref.	$Fe(2p_{1/2})$	$Fe(2p_{3/2})$	Fe(3s)	Fe(3p)	O(1s)
[22]	–	709.7	–	–	530.3
[10]	723.8	710.3	–	–	530.1
[11]	723.0	709.4	–	–	–
[12]	722.8	709.5	92.5	53.7	529.2
[13]	–	709.7	–	–	–
[21]	–	709.5	92.5	54.9	530.0
[32]	722.8	709.5	92.3	53.7	529.7

Binding energy data for Fe_3O_4

Ref.	$Fe(2p_{1/2})$	$Fe(2p_{3/2})$	Fe(3s)	Fe(3p)	O(1s)
[10]	724.9	711.4	–	–	530.1
[11]	722.6	710.2	–	–	–
[17]	723.8	710.8	–	55.9	–
[20]	724.0	710.9	93.6	56.2	530.2
[32]	–	710.3	–	–	529.9
[33]	724.4	710.6	–	–	–
[22]	–	709.5/711.2	–	–	530.3
[16]	–	709.3/711.0	–	–	–
[12]	722.8/724.0	709.5/710.5	92.4/93.2	54.9/55.8	529.1

Binding energy data for Fe_2O_3

Ref.	$Fe(2p_{1/2})$	$Fe(2p_{3/2})$	Fe(3s)	Fe(3p)	O(1s)
[22]	–	711.2	–	–	530.3
[10]	724.6	711.4	–	–	530.2
[11]	724.1	710.5	–	–	–
[12]	723.8	710.3	93.0	55.3	529.3
[13]	–	711.2	–	–	–
[20]	724.3	711.0	93.8	55.8	530.0
[21]	–	711.0	93.6	55.7	529.8
[32]	–	710.6	–	–	530.0
[33]	723.6	710.3	93.1	55.2	529.3
[34]	725.0	711.4	–	–	–

Single values indicate positions of iron core-level peak maxima Fe(II)/Fe(III) binding energies are both given where reported.

In experimentation, it was found that the Fe-K (Fe/K ~ 55) and Fe-Cu catalysts carborized completely upon exposure to reactants ($CO/H_2 = 1/3$) at 250 °C for 3 h. In addition, K and Cu had no detectable effect on the kinetics of carburization or the structure of the carbide. However, Ni and Co both had pronounced effects on carburization. The alloying with Co completely suppressed carbide formation under these conditions, with the Mössbauer pattern of the FT alloy corresponding to that of a sample that had simply been reduced in H_2, 425 °C, 24 h. A broadening of the peaks in the pattern indicated the formation of a rather inhomogeneous bcc Fe-Co alloy. The Fe-Ni under the same conditions carburized rapidly (a steady state composition was attained after 1.5 h), but incompletely. The material resulting from FT conditions is very complex; in addition to a carbide phase, a major component of iron-rich bcc alloy remains together with a small amount of a fcc alloy phase. The carbide phase formed also differs from the expected phase of ε'-$Fe_{2.2}C$; Mössbauer patterns suggest that a

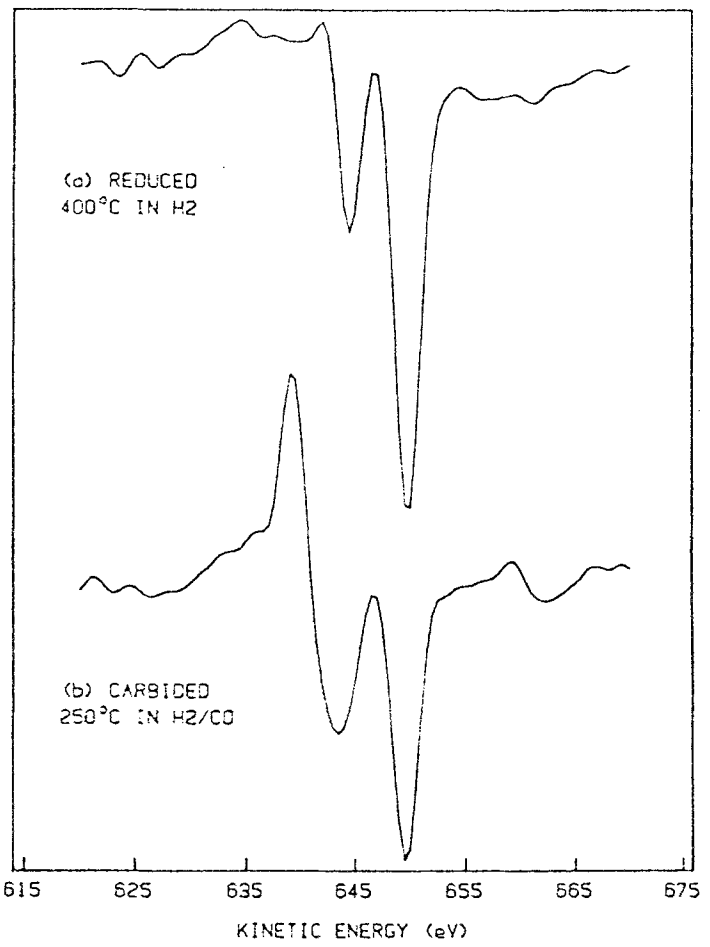

Fig. 5. Derivative LMV Auger transition spectra for reduced and carbided iron powders.

mixed Fe-Ni carbide phase is formed, similar to that reported for some meteors [21,22]. Carbide formation in the Fe-Ni system seems sensitive to morphology and composition since Raupp and Delgass [2] report no carburization in a Fe/Ni = 1 catalyst on SiO_2, where the particles were found to be a single phase alloy and were considerably smaller than in [19].

The simple recital of whether or not carbide phases are formed, what alloys are formed, and stabilities under FT reaction conditions is interesting and necessary, but is a rather sterile exercise in the absence of any correlation with reaction activity and selectivity data. Some aspects of this are examined in the next section, and in detail in Part II.

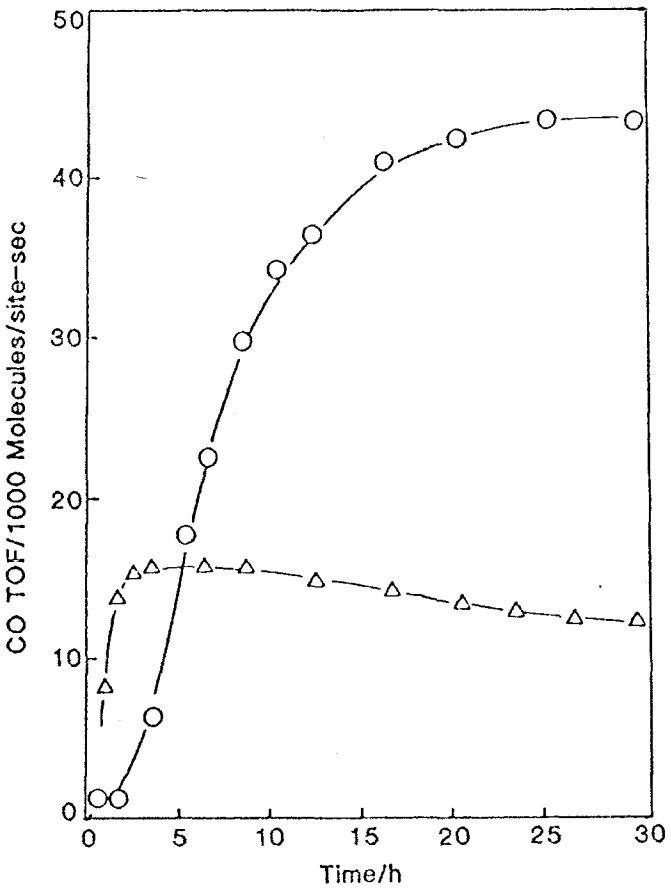

Fig. 6. a) CO turnover vs. time in the XPS cell at 1% conversion. ○ – unreduced oxide powder, △ – reduced oxide powder. b) Example of Fe (2p) spectrum fitting after synthesis for 2 h. The top curve is that experimentally observed. The second curve is for iron metal; the third for iron carbide. Overall composition of this sample was 62.4% metal, 37.4% carbide, 0.2% oxide.

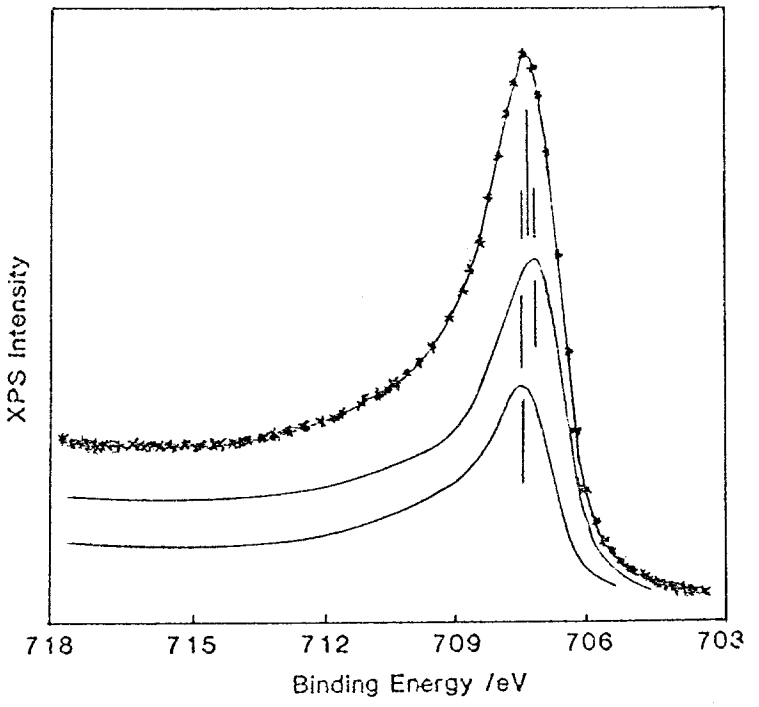

Fig. 6. (continued).

4. Selected surface studies of iron

To this point all the characterization studies (i.e., Mössbauer, X-ray, etc.) discussed are bulk methods that are not surface-sensitive, and, thus provide little information about the chemical nature of the iron surface (or of surfaces formed) during synthesis. Much of the surface studies that has been done has focused on characterization of carbonaceous deposits formed during synthesis, which is necessary information for examining the surface aspects of carbide formation. Bonzel and Krebs [23] proposed three forms of surface carbon on iron: a "CH" (hydrocarbon phase) and a partially hydrogenated "carbide carbon" phase were identified in the early stages of the synthesis reaction and were associated with a rapid increase in the methanation activity (c.f., fig. 1). At longer reaction times the formation of a "graphitic carbon" phase, associated with a steady decrease in activity, was identified.

Detailed characterization of the nature of iron-based FT catalysts, and the role of carbide phases, depends on the availability of reliable XPS spectral data for iron, iron oxides and iron carbides. A convenient summary of these data for the metal and oxides through 1988 has been presented by Kuivila et al. [5], and is given in table 4. (References in the table are given in [5].) There are some useful guides to interpretation of these spectra [24]:

Table 5
Core level binding energies of iron phases

	Fe	Fe_5C_2	Fe_3O_4	Fe_2O_3
Fe ($2p_{1/2}$)	720.0	720.3	724.0	724.8
Fe ($2p_{3/2}$)	707.0	707.3	710.8	711.2
Fe (3s)	90.8	91.4	92.6	93.6
Fe (3p)	52.4	53.0	55.0	55.6
O (1s)	–	–	530.3	530.3
C (1s)	–	283.2	–	–

(1) Fe(III) has a $2p_{3/2}$ binding energy of 711.2 eV in all iron oxides (Fe_2O_3, Fe_3O_4, FeOOH), and Fe(II) has a binding energy of 709.7 eV in Fe_xO.

(2) Octahedrally and tetrahedrally coordinated Fe(III) species cannot be distinguished by their core-level XPS spectra.

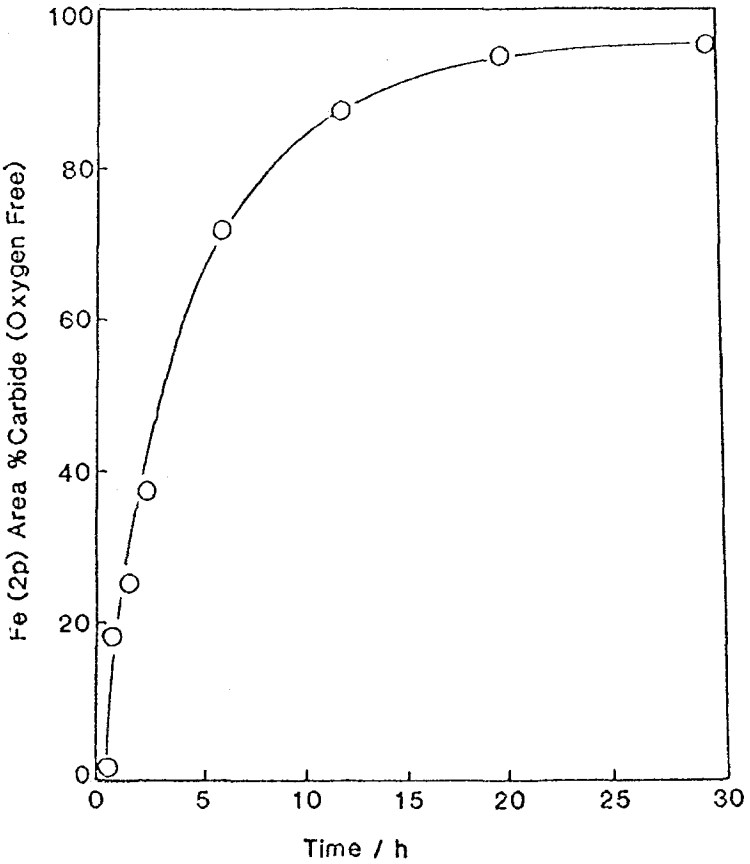

Fig. 7. a) Carbide contributions to the Fe (2p) XPS spectra of the reduced, unsupported catalyst as a function of time of reaction. b) C(1s) peak area as a function of time of reaction for the reduced, unsupported catalyst.

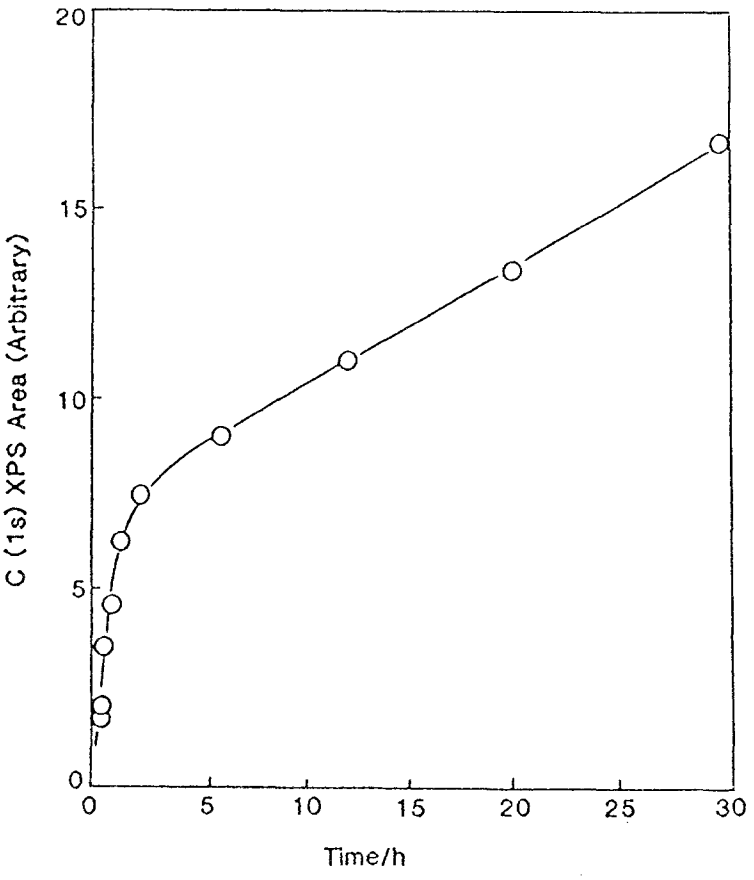

Fig. 7. (continued).

(3) Since Fe(II) and Fe(III) are in the high spin states, unresolved multiple splitting leads to broad iron core-level spectra for the oxides.

(4) A broad shake-up satellite centered at 719.8 eV is characteristic of Fe(III), independent of oxide or coordination, and a satellite at ~ 715 eV is characteristic of a Fe(II) species.

(5) The Fe(2p) spectrum of Fe_3O_4 is characterized by an apparent lack of satellite structure, which is actually the result of superpositioning of the Fe(II) and Fe(III) satellites.

(6) The Fe_3O_4 spectrum is essentially a weighted average of spectra for Fe_xO and Fe_2O_3. Subtraction of the Fe_2O_3 spectrum from Fe_3O_4 gives an Fe(II) peak at 709.5 eV, in good agreement with results for Fe_xO.

(7) The O(1s) binding energy for all iron oxides is 530.3 eV, making it of little value for discriminating among compounds. An O(1s) peak at ~ 532 eV is characteristic of adsorbed OH.

In contract to the oxides, the literature on carbides is less abundant. The most pertinent data are given in refs. [5] and [25], and a summary of the core level

binding energy data most useful for distinguishing between the different chemical states of iron in synthesis catalysts is given in table 5. Fig. 3 shows spectra obtained for carburized powder samples, along with the corresponding metallic Fe spectra. An Fe ($2p_{3/2}$) binding energy of 707.0 eV for reduced Fe is reproducibly shifted to 707.3 eV upon carburization. It is of interest to point out that the carbide of the H_2/CO sample (3 : 1) was identified by Mössbauer to correspond to essentially 100% χ-Fe_5C_2 [5], while that corresponding to the ethylene carburization (pure C_2H_4, 1 atm) consisted of 62% χ-Fe_5C_2 and 38% Θ-Fe_3C. Carbon core level measurements are also of interest in the characterization of carbide phases, and a C(1s) spectral comparison is shown in fig. 4. The major peak in spectrum (b) here at 284.6 eV, is that due to "graphitic" carbon (which may also include adsorbed hydrocarbon products and surface precursors to products). Moderate sputtering in Ar is sufficient to remove this "graphitic" layer from the surface, revealing the characteristic Fe carbide peak at 283.2 eV, in this case identified with Haag carbide, χ-Fe_5C_2.

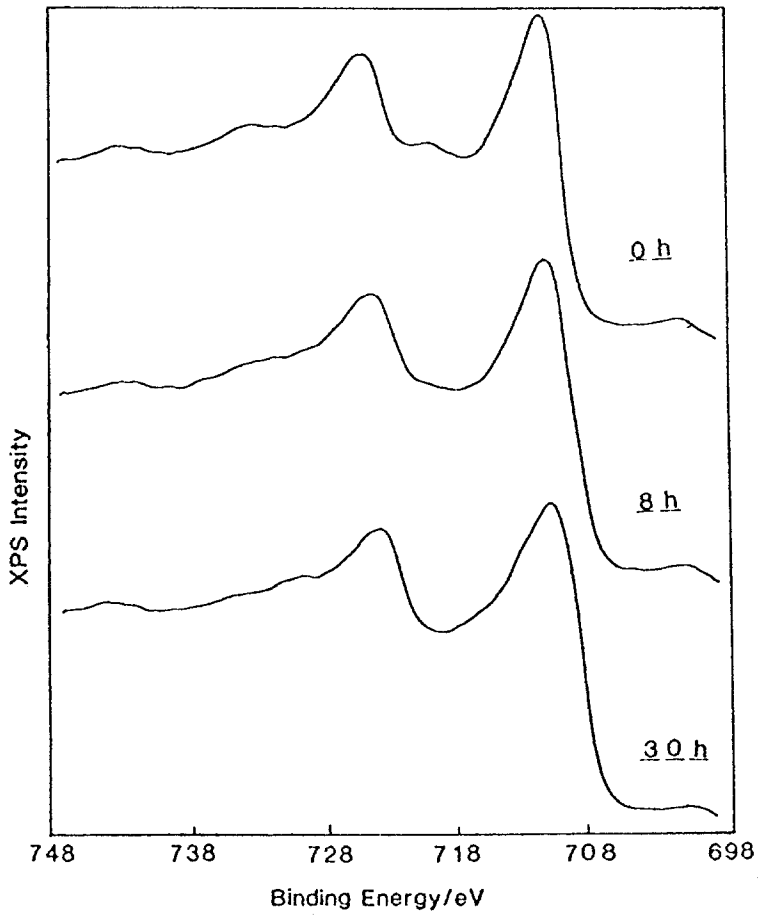

Fig. 8. Fe (2p) spectra of unreduced oxide powder as a function of synthesis time.

Carbides can also be distinguished from other forms of iron by differences in the iron Auger spectra, as shown in fig. 5. Differences in line shapes are most pronounced for the Fe (LMV) Auger transition, which appears in the kinetic energy range 620–660 eV. For Al Kα radiation (used in [5]) this region includes the Fe(2s) core transition at 639 eV. The ratio of maximum to minimum values for the metallic iron spectrum is 0.14, compared to a ratio of 0.71 for the carbided sample, suggesting that this ratio can be used to follow the formation of surface carbide phases. Overall, of course, the more general problem of interest in FT catalysis is the analysis of surfaces that do not consist of a single phase. This can be done by determining the relative contributions of the individual iron oxidation states and iron carbide to the Fe(2p) XPS spectrum using a linear combination of least squares fits to standard iron core level spectra for Fe, Fe(II), Fe(III) and Fe_5C_2 (figs. 4 and 7 in ref. [5]).

The application of these methods to study of the behavior of both prereduced and unreduced iron catalysts under FT conditions in $CO/H_2: 3/1$ at 1 atm and 250 °C is given in [26], following earlier investigations [25,27] indicating that carbide phases were indeed formed within the surface region of Fe foils under FT conditions. Data on CO turnover frequency for reaction on powder catalysts at low conversion are shown in fig. 6a; these reactions were conducted in an XPS/reactor system whose behavior was shown [26] to be similar to that of a conventional fixed-bed reactor. Typical results for the reduced powder after brief exposure to synthesis conditions, in terms of the Fe ($2p_{3/2}$) transition, are shown in fig. 6b and indicate the utility of the multicomponent spectral fitting procedure. The carbide contributions to the Fe(2p) spectrum and the C(1s) peak area, both as a function of time are given in fig. 7. The carbide contributions, fig. 7a, are calculated as the percentage of carbide associated with the reduced metal phase (metal plus carbide) on an oxide-free basis. It is seen that the spectrum does not change appreciably after 15 h, maintaining a small metallic iron contribution ($\sim 5\%$). The carbon peak area reflects the fact that graphitic carbon increases steadily with time-on-stream. Both carbidic and graphitic carbon accumulate rapidly during the first few hours of synthesis, and this initial rapid accumulation of surface carbon coincides with increasing synthesis activity. The increase of graphitic carbon at longer reaction times, however, has little influence on overall synthesis activity, at least as measured by CO turnover (c.f., fig. 6a).

The course of synthesis starting with an unreduced iron oxide as the catalyst presents a different and interesting story. It is apparent, also from fig. 6a, that the oxide possesses CO conversion activity * that grows in after an induction period of several hours. Core level iron XPS spectra measured during the course of

* Quantitative comparison of the levels of activity is tricky. For the sake of consistency the specific reaction rates of fig. 6a were calculated on the basis of hydrogen uptake of the reduced powder. Although this hydrogen uptake is not meaningful for the unreduced oxide, the reaction rates are put on a consistent basis (per gram of catalyst) with reference to the reduced powder.

reaction are shown in fig. 8. The initial spectrum exhibits features characteristic of Fe_2O_3, with subsequent disappearance of the Fe(III) satellite peak at 719 eV (8 h) and broadening of the parent peak signaling a partial reduction to divalent iron. The final spectrum (30 h) is essentially that of Fe_3O_4 with *no* discernable metal *or* carbide contributions. Carbon core level measurements were also significantly different from those for the reduced materials; all C(is) spectra were narrow with peak maxima corresponding to graphite carbon alone and *no* significant carbidic contribution ($\sim$ 5%). Unfortunately, there is some disagreement [26] with Mössbauer results on this point, which indicate the presence of about 20% Fe_5C_2. However, the fact remains that a quite active FT catalyst can be produced in which carbides phases are minor constituents. In fact, the possible FT activity of Fe_3O_4 had been pointed out by Reymond et al. [28], though not without dispute [29].

A summary of changes in near-surface composition, and a comparison of carbon build-up on the reduced and unreduced materials is given in fig. 9. It is seen that the rates of carbon accumulation are quite different. The higher

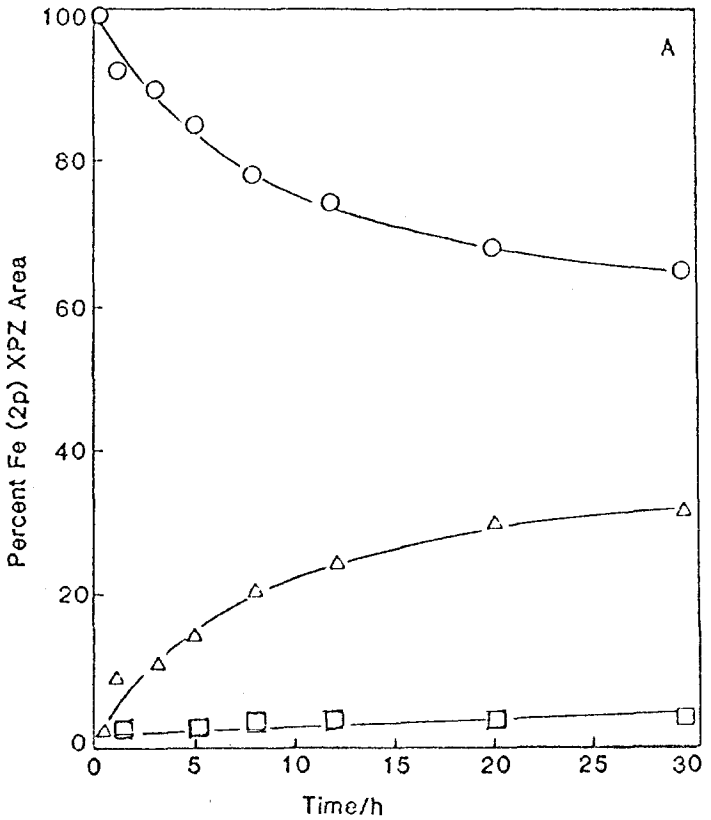

Fig. 9. (A) Survey of near-surface composition vs. time of reaction for the unreduced oxide powder. ○ – Fe^{3+}, △ – Fe^{2+}, □ – carbide (B) Comparison of C(1s) peak areas in reduced and unreduced catalysts. ○ – reduced oxide, △ – unreduced oxide.

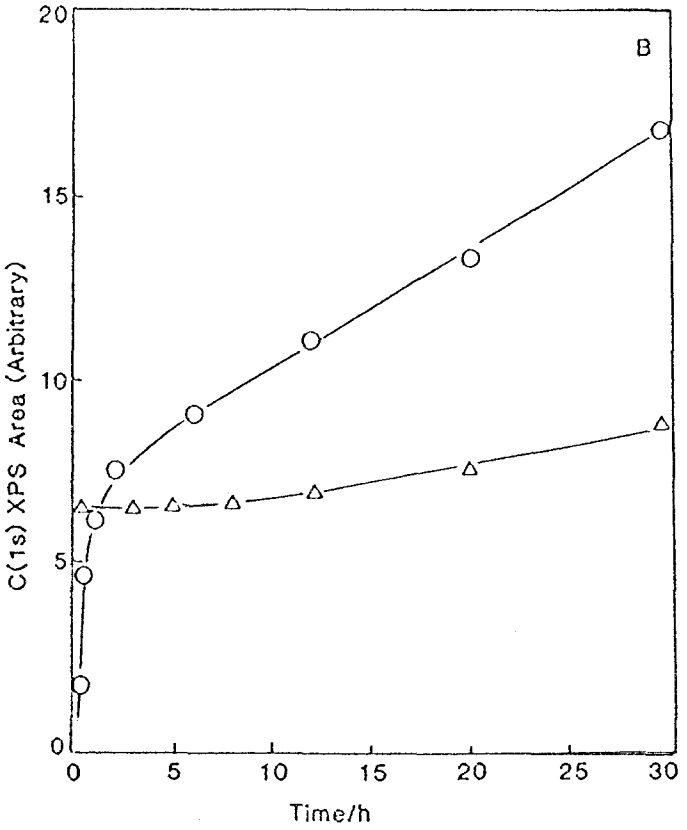

Fig. 9. (continued).

steady-state synthesis activities seen for the initially unreduced catalysts may be explained by a combination of smaller amounts of inactive surface carbon and the steady activation resulting from the progressive reduction from Fe_2O_3 to Fe_3O_4. It would not appear that carbide formation is associated with the higher rates of deactivation of reduced iron catalysts [60], since the activation of reduced iron is clearly associated with carbide formation ([1–3,26] among many others). Rather, it seems clear at lower pressures, reduced iron catalysts are more susceptible to the accumulation of graphitic surface carbon (quite distinct from carbide), which is responsible for the deactivation.

Separate experiments reported [26] for higher conversion levels (~ 40% total CO) alter details of the picture above, but do not change the overall picture. The rate of carbide formation is retarded, probably due to product inhibition by water [30], and the extent of graphitic carbon formation is decreased. If graphitic carbon is indeed the agent responsible for catalyst deactivation, then the rate of deactivation of a catalyst operating in an intermediate conversion environment should be smaller than that of one operating in the low conversion environment. This is the case for the reduced catalyst operating at 40% CO conversion shown in

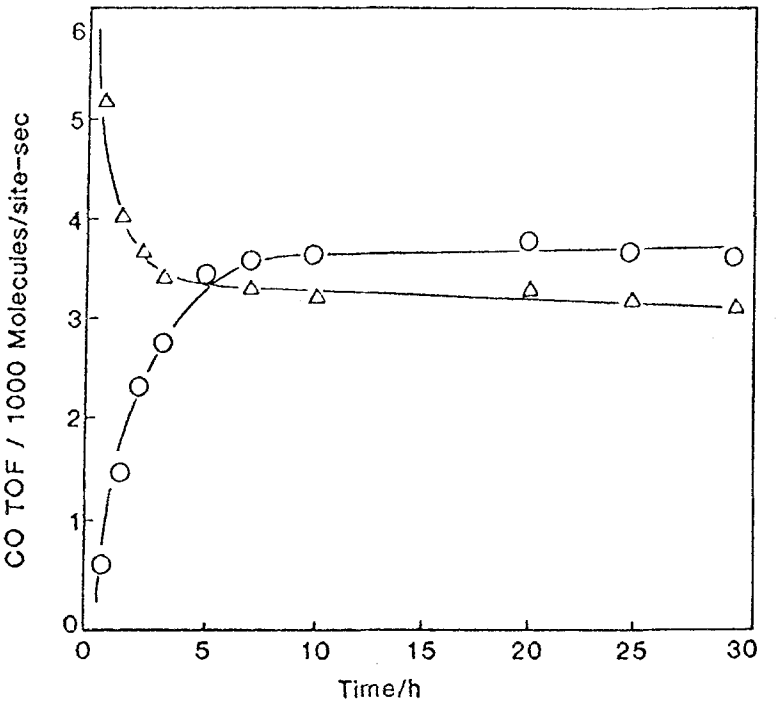

Fig. 10. CO turnover frequency for the reduced oxide powder at intermediate conversion (prereactor and XPS cell in series). ○ – to hydrocarbons, △ – to CO_2.

fig. 10. The turnover both the hydrocarbons and CO_2 is seen to be quite stable with respect to time-on-stream (c.f., fig. 6a). Overall, while carbide has been shown to enhance the competitive chemisorption of H_2 over C [16], and this may be at least in part responsible for the initial activation of reduced iron, it is not clear that this is a dominant effect in long term, high-conversion operation.

5. Summary

The characterization studies surveyed here demonstrate that the initial activation of reduced iron appears well correlated with the formation of a carbide phase. However, it can be argued that this is due more to a promotion than a geometric (i.e., site formation) effect. Surface studies are in general accord with characterizations via other methods as to the formation of carbide phases, but the role of surface carbon species in long-term activity maintenance remains elusive. Finally, the activity of materials such as Fe_3O_4, where carbide phases are minor constituents of the working catalyst, leads to additional questions as to the role of carbides in determination of activity and selectivity. These questions are addressed more directly in the reaction studies of Part II.

References

[1] J.A. Amelse, J.B. Butt and L.H. Schwartz, J. Phys. Chem. 82 (1978) 558.
[2] G.B. Raupp and W.N. Delgass, J. Catal. 58 (1979) 348, 361.
[3] J.W. Niemantsverdriet, A.M. van der Kraan, W.J. van Dijk and H.S. van der Baan, J. Phys. Chem. 84 (1980) 3363.
[4] K.M. Sancier, W.E. Isakson and H. Wise, *Advances in Fischer-Tropsch Chemistry*, ACS Anaheim Meeting (1978) p. 545.
[5] C.S. Kuivila, J.B. Butt and P.C. Stair, Appl. Surf. Sci. 32 (1988) 99.
[6] D.J. Dwyer and G.A. Somorjai, J. Catal. 52 (1978) 291; 56 (1978) 249.
[7] A.J. Krebs, H.P. Bonzel and G. Gafner, Surf. Sci. 88 (1979) 269.
[8] R.A. Arents, Yu. V. Maksimov, I.P. Suydalev, V.K. Imshennik and Yu. F. Krupyanskiy, Fiz. Metal. Metallovred. 36 (1973) 277.
[9] S. Nagahura, J. Phys. Soc. Japan 14 (1959) 186.
[10] L.J.E. Hofer, E. Sterling and J.T. McCartney, J. Phys. Chem. 59 (1955) 1153.
[11] R.B. Anderson, in: *Catalysis*, ed. P.H. Emmet, Vol. IV (Reinhold, NY, 1956).
[12] J.A. Amelse, G. Grynkewich, J.B. Butt and L.H. Schwartz, J. Phys. Chem. 85 (1981) 2484.
[13] H. Kundig, H. Bommel, G. Constabaris and R.H. Lindquist, Phys. Rev. 142 (1966) 327.
[14] S.M. Loktev, L.I. Makarenkova, E.V. Slivinskii and S.D. Entin, Kin. i Katal. 13 (1972) 933.
[15] H. Pichler, Adv. Catal. 4 (1952) 271.
[16] R.J. Matyi, L.H. Schwartz and J.B. Butt, Catal. Rev.-Scie. Engr. 29 (1987) 41.
[17] M.E. Dry, T. Shingles, L. Boshoff and A. Vosthuisen, J. Catal. 15 (1969) 190; see also: M.E. Dry and G.J. Oosthuizen, J. Catal. 11 (1968) 18.
[18] M.A. Vannice and R.L. Garten, Paper 17e, 67th AIChE Meeting, Washington, D.C., December 1974.
[19] J.A. Amelse, L.H. Schwartz and J.B. Butt, J. Catal. 63 (1981) 95.
[20] H.J. Goldschmidt, *Interstitial Alloys* (Plenum, New York, 1967).
[21] E. Unmuth, L.H. Schwartz and J.B. Butt, J. Catal. 63 (1980) 404.
[22] A.D. Romig and J.I. Goldstein, Metall. Trans. A 92 (1978) 1599.
[23] H.P. Bonzel and H.J. Krebs, Surf. Sci. 91 (1980) 499.
[24] K. Wandelt, Surf. Sci. Rept. 2 (1982) 1.
[25] D.J. Dwyer and J.H. Hardenbergh, J. Catal. 87 (1984) 66.
[26] C.S. Kuivila, P.C. Stair and J.B. Butt, J. Catal. 118 (1989) 299.
[27] D.J. Dwyer and J.H. Hardenbergh, Appl. Surf. Sci. 19 (1984) 14.
[28] J.P. Reymond, P. Meriandeau and S. Teichner, J. Catal. 75 (1982) 39.
[29] R.A. Dictor and A.T. Bell, J. Catal. 97 (1986) 121.
[30] J.F. Schultz, W.K. Hall, B. Seligman and R.B. Anderson, J. Am. Chem. Soc. 77 (1955) 213.